CHEMISTRY OF MATERIALS

ARTICLE

pubs.acs.org/cm

Preparation, Photophysical, Electrochemical, and Sensing Properties of Luminescent Tetrazine-Doped Silica Nanoparticles

Jeremy Malinge, Clémence Allain,* Laurent Galmiche, Fabien Miomandre, and Pierre Audebert*

PPSM, ENS Cachan, CNRS UMR8531, 61 av President Wilson, F-94230 Cachan, France

Supporting Information

ABSTRACT: Luminescent hybrid silica nanoparticles grafted with tetrazines fluorophores have been synthesized and characterized, and their photophysical and electrochemical properties have been studied in acetonitrile solutions. The photophysical behavior of the functionalized nanoparticles shows a bright fluorescence emission, with emission and excitation bands typical of chloroalkoxytetrazines fluorophores, albeit with some degree of quenching because of interchromophoric interactions. Their fluorescence emission properties have been studied in the presence of various low molecular weight amines. Extinction of the fluorescence of the nanoparticles because of photoinduced electron transfer between the photoexcited tetrazine and the amine is observed, making these functionalized nanoparticles potentially useful for amine sensing.

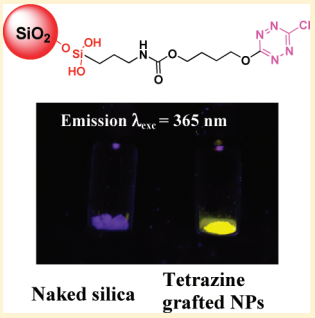

KEYWORDS: fluorescence, silica nanoparticles, tetrazines, electrochemistry, fluorescent sensor

INTRODUCTION

Luminescent silica nanoparticles are versatile nanoobjects with many appealing features:[1] silica is photophysically inert and not intrinsically toxic, and monodisperse nanoparticles can easily be prepared and functionalized under mild conditions following the Stöber methodology[2] and its modification by Van Blaaderen and Vrij[3] or using the reverse microemulsion method.[4] A large number of fluorescent dyes can be hosted in the relatively small volume of a nanoparticle, allowing the formation of ultrabright nanoobjects. Silica nanoparticles also constitute a platform to prepare self-organized[5] or multicomponent architectures[6] with complex photophysical properties. This type of nanoparticles has thus been applied to solve important analytical problems, in the field of biomedical imaging or diagnostics[7] as well as for the design of nanoswitches[8] and nanosensors. While in some cases self-quenching of the fluorophores embedded in silica nanoparticles have been observed,[9,10] sensors with an amplification of the fluorescence response toward a targeted analyte have also been reported.[11−13] Functionalized luminescent silica nanoparticles are also particularly suitable for the design of fluorescent sensors because they can be either dispersed in organic or aqueous solutions and easily collected and reused by sequential centrifugations and washings, or studied as solid-state arrays.[14]

s-Tetrazines are highly colored (because of a low-lying π^* orbital leading to a n-π^* transition in the visible) and electroactive heterocycles that display a very high electron affinity.[15,16] These molecules have been widely used as dienes in inverse electron demand Diels−Alder reactions,[17] and to develop nitrogen-rich energetic materials.[18] We[19−21] and others[22] evidenced that some tetrazines substituted with heteroatoms displayed a high fluorescence quantum yield together with a good chemical and photochemical stability. The fluorescence properties of tetrazines, associated with their small size and their strong electron-deficient character, make these dyes very attractive for sensing applications: as tetrazines, in their ground state and even more in their first excited state, have a strong oxidizing power, and their fluorescence is quenched by various electron donors.[19,23]

Tetrazines thus constitute a promising family of compounds for the detection of electron-rich pollutants, such as aliphatic or aromatic amines. The detection of low-molecular weight amines is of importance in medical diagnostics, in food safety, and in environmental monitoring. Consequently, the design of amine responsive fluorophores[24] is of interest as it can lead to the development of inexpensive, real-time, portable, and sensitive sensors. We describe here the synthesis, photophysical and electrochemical properties of silica nanoparticles grafted on their surface with tetrazine dyes. The fluorimetric sensing of amines by these nanoparticles has also been investigated.

RESULTS AND DISCUSSION

Synthesis of Luminescent Nanoparticles. Nucleophilic aromatic substitution on the versatile synthon 3,6-dichlorotetrazine[20] by the alcohol group of compound **1** (prepared by reaction between 1,4-butanediol and triethoxy(3-isocyanatopropyl)silane) provided the tetrazine dye bearing a triethoxysilane group **2** (Scheme 1) in good yield. To investigate the influence of the distance between the tetrazine ring and the surface of the nanoparticle, we also reacted the alcohol **3** bearing a longer spacer with 3,6-dichlorotetrazine to obtain tetrazine **4**. Silica nanoparticles were prepared using the Stöber method and characterized by dynamic light scattering (DLS) and scanning electron microscopy

Received: July 31, 2011
Revised: September 16, 2011
Published: September 29, 2011

Scheme 1. Synthesis of Tetrazine-Silane Fluorophores 2 and 4

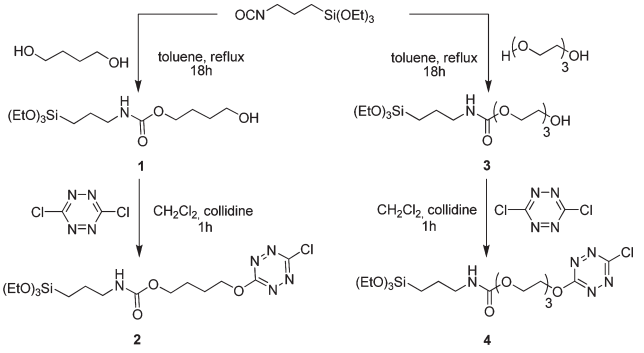

Table 1. Diameter (DLS and SEM) and Composition (Elemental Analysis) of the Nanoparticles

	diameter (nm)		composition		
system	DLS	SEM	%C	%H	%N
NP0	135	97			
NP1	148	106	3.5	1.6	1.8
NP2	155		6.9	1.7	2.4

(SEM) to measure their diameter (Table 1) and check their monodispersity (Supporting Information, Figure S1). As reported in the literature, monodisperse nanoparticles, **NP0**, have been obtained, and the diameter measured by SEM is smaller than the diameter measured by DLS, which has been attributed to shrinkage of the particles under the electron beam.[25]

The nanoparticles **NP0** were then grafted with tetrazines **2** or **4** under mild acidic conditions to yield respectively tetrazines-doped nanoparticles **NP1** ("short" tetrazine-silica spacer) and **NP2** ("long" spacer). Aliquots of nanoparticles **NP1** were analyzed by fluorescence spectroscopy at regular time intervals during the grafting reaction. A marked increase of the fluorescence emission intensity was observed during the first 24 h of the grafting reaction, then the fluorescence emission intensity reached a plateau (Supporting Information, Figure S2). The grafting reaction was stopped after 24 h, and the nanoparticles were purified by repeated centrifugations and washings. DLS and SEM analysis (Table 1) showed that for both grafting reactions the nanoparticles became slightly bigger after grafting, and that their size remained monodisperse (Figure 1 shows an image of grafted nanoparticles **NP1**). The amount of tetrazines grafted per nanoparticle was evaluated using elemental analysis. Values of 0.26 mmol and 0.34 mmol of tetrazine per gram of silica nanoparticle were calculated for **NP**1 and **NP2**, respectively. These values are comparable to the highest values reported in the literature for nanoparticles similar in size,[9] and similar amounts of grafted dyes have also been reported for smaller nanoparticles with a higher surface to volume ratio.[26]

Photophysical Properties. The spectroscopic properties of the nanoparticles as suspensions in acetonitrile were investigated and compared to those of precursor tetrazine **2**. Tetrazine **2** displays spectroscopic properties typical of a chloroalkoxytetrazine with two absorption bands (λ_{abs}= 330, 515 nm in acetonitrile) and an intense (ϕ = 0.26 in acetonitrile) and broad fluorescence emission around 560 nm (Figure 2.). Because of the

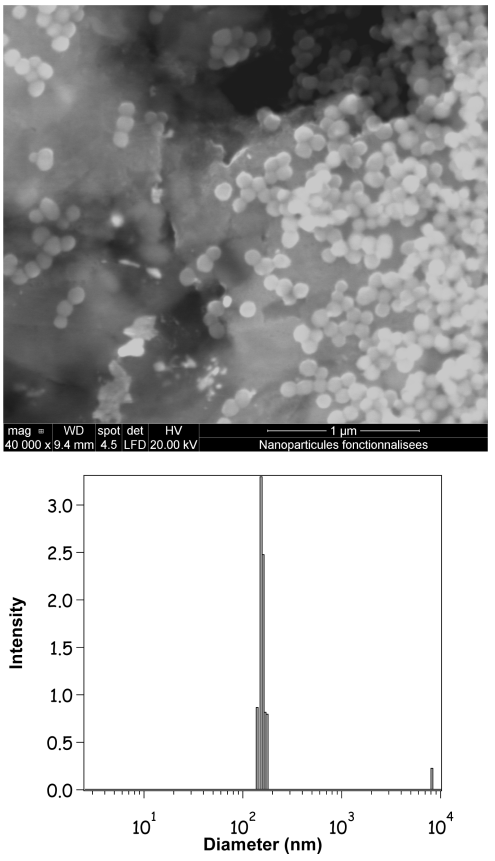

Figure 1. SEM image and size distribution measured by DLS of tetrazine functionalized nanoparticles.

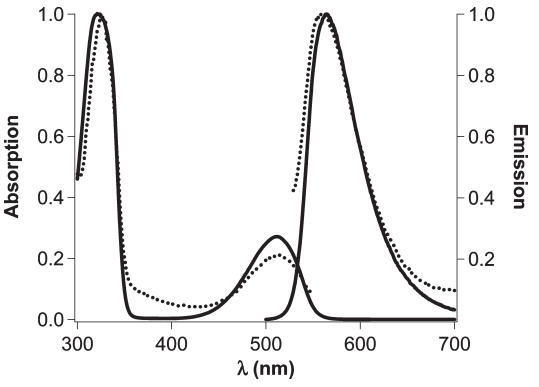

Figure 2. Absorption and emission spectra of tetrazine **2** in solution (CH3CN) (full lines) and excitation and emission spectra of functionalized nanoparticles (**NP1** or **NP2**) (dotted lines).

forbidden nature of the n-π^* transition responsible for the fluorescence, tetrazines **2** and **4** display very long fluorescence lifetimes (τ = 148 ns for **2** and τ = 156 ns for **4**) in acetonitrile solutions (Figure 3), as already reported for chloroalkoxytetrazines.[15]

Dispersions of tetrazine doped nanoparticles **NP1** and **NP2** in acetonitrile strongly scatter light, which makes impossible the measurements of molar extinction coefficients. However, comparison of the UV−vis extinction spectra of tetrazine **2** with doped nanoparticles (Supporting Information, Figure S3) shows that the grafting of tetrazine on silica does not induce any shift in

dx.doi.org/10.1021/cm202223w |*Chem. Mater.* 2011, 23, 4599–4605

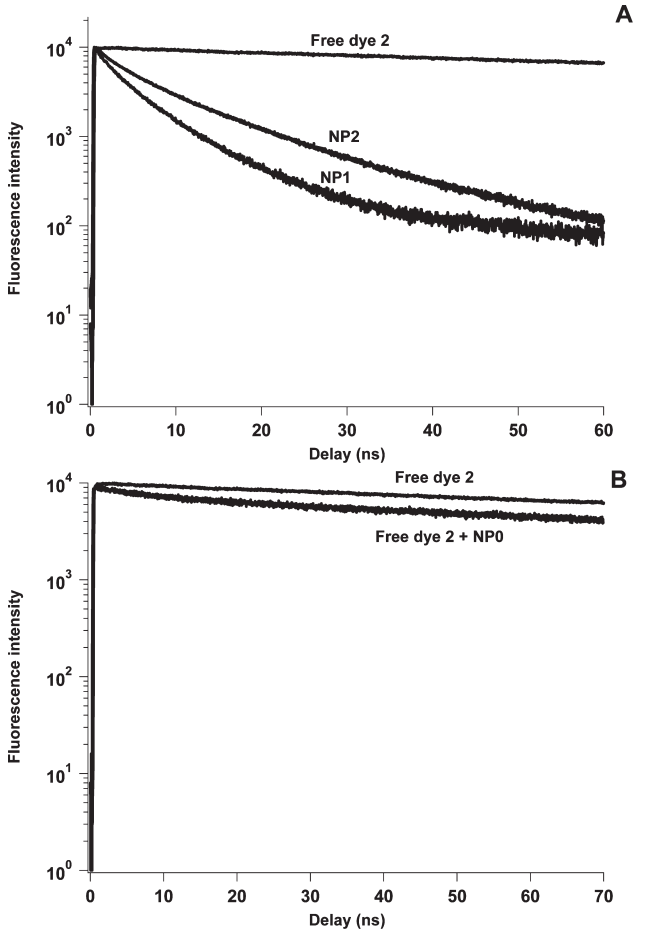

Figure 3. (**A**) Fluorescence decays of free dye **2**, **NP1**, and **NP2** in CH_3CN. (**B**) Fluorescence decays of free dye **2** and **NP0** + free dye **2** (excitation wavelength 495 nm).

the absorption maxima for **NP1** or **NP2**. This confirms the absence of interactions between grafted tetrazine dyes in their ground state. Steady-state fluorescence emission spectra of the nanoparticles **NP1** and **NP2** are similar to the one of tetrazine **2** (Figure 2), indicating that the immobilization of tetrazines onto silica nanoparticles does not lead to the formation of luminescent aggregates such as excimers or J-aggregates.

Time resolved spectroscopy indicates an interesting feature of our system. While the free dye **2** in solution exhibits a long fluorescence lifetime that can be fitted with a monoexponential decay, functionalized nanoparticles show a different behavior. Multiexponential decays are observed for both **NP1** and **NP2** with an average excited state decay time of 4.83 and 12.24 ns, respectively (Figure 3A and Supporting Information). This indicates that the emitted light comes from fluorophores in various environments. To investigate possible interactions between the tetrazine ring and the silica surface, the fluorescence decay of a suspension of **NP0** in CH_3CN together with free dye **2** was recorded and compared with the free dye alone (Figure 3B). From those results one can say that interactions occur between tetrazine and silica, slightly shortening the lifetime decay. Furthermore, the fluorescence decay of **NP1** was compared with the one of free dye **2** mixed with naked silica nanoparticles **NP0**. This highlights that interactions between tetrazines grafted on the nanoparticles occur and lead to self-quenching. This is consistent

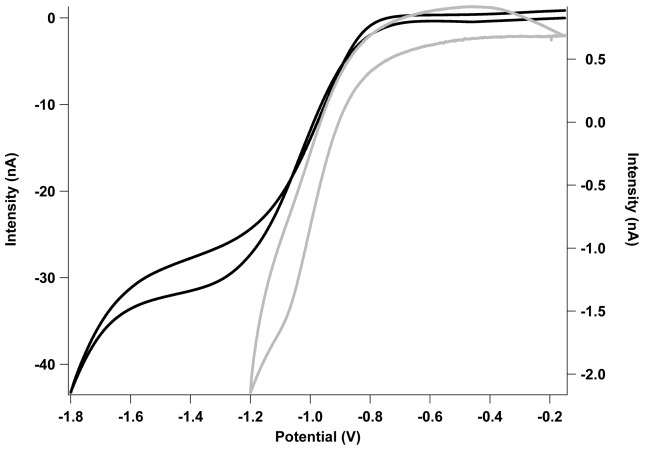

Figure 4. Cyclic voltammetry of **NP1** suspension (gray curve, right scale) in acetonitrile without supporting electrolyte ([Tz] ≅ 0.6 mM) using a Pt ultramicroelectrode (r = 50 μm) as the working electrode. Comparison with ungrafted tetrazine **2** (black curve, left scale) in the same conditions. Potentials vs Ag^+/Ag.

with previous observations: although tetrazines are known to remain fluorescent in the solid state, time-resolved fluorescence measurements on chloroalkotetrazine crystals have evidenced a decrease of the fluorescence lifetime compared to solution because of intermolecular interactions between tetrazines.[19]

This quenching phenomenon is more important in the case of **NP1** where the distance between the tetrazine core and the silica surface is shorter, despite a slightly lower amount of dye per nanoparticle for **NP1** than for **NP2**. This suggests that the length of the spacer in the case of **NP1** yields a denser layer of fluorophores on the nanoparticles, leading to amplification of tetrazine interchain self-quenching event. On the other hand, with a longer spacer (**NP2**), the average fluorescence lifetime is longer, suggesting that tetrazines behave more like free dyes than aggregated fluorophores.

Electrochemical Properties. The electrochemical behavior of **NP1** was investigated on an ultramicroelectrode without supporting electrolyte to avoid flocculation phenomena induced by increase of the ionic strength. Figure 4 displays the resulting cyclic voltammogram showing the classical waves associated to radial diffusion. Compared to the parent tetrazine **2** it can be noticed that reduction occurs in a single wave at nearly the same potential, which confirms that redox species behave in a similar way in the nanoparticle and in the solution.

The limiting current i' is related to the concentration of electroactive species C according to the following equation for a disk ultramicroelectrode of radius r:

$$i' = 4nFDrC \tag{1}$$

where n is the number of exchanged electrons per redox species and D is the diffusion coefficient. Using the ratio of limiting currents for **NP1** and **2** allows us to get rid of the actual electrode radius and leads to

$$C_{NP1} = C_2 \frac{i'_{NP1}}{i'_2}\frac{D_2}{D_{NP1}} = C_2 \frac{i'_{NP1}}{i'_2}\frac{d_{NP1}}{d_2} = \frac{2}{33}\frac{150}{2.1} = 4.3C_2 \tag{2}$$

where d is the hydrodynamic diameter.

dx.doi.org/10.1021/cm202223w |*Chem. Mater.* 2011, 23, 4599–4605

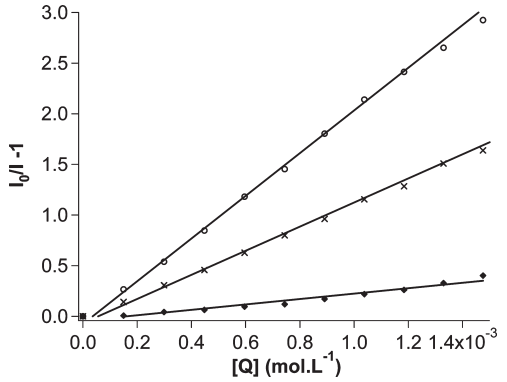

Figure 5. Stern−Volmer plots for the free dye **2** as function of quencher concentration for various quenchers: ○ **DPA**; ◆ **EtOA**; × **TEA** (excitation wavelength 340 nm).

According to the amount of tetrazine in the NPs predicted from elemental analysis, the concentration ratio should be equal to 1. Equation 2 leads to an overestimated value, probably because of an additional contribution coming from migration, as evidenced by the variation of the plateau current upon addition of small amounts of electrolyte salt. However the results tend to show that the major part of (if not all) the tetrazine units incorporated in the nanoparticle are actually electroactive, which is often a crucial issue in redox functionalized silica nanoparticles as previously reported by Murray and Speiser in the case of ferrocene.[27] In that case it could be inferred that tetrazines are mainly located near the NP surface, otherwise a much lower current for the functionalized NPs would be expected.

Sensing Properties. In a first step, fluorescence quenching experiments were performed with tetrazine **2** and aliphatic or aromatic amines: the effect of the addition of diphenylamine (**DPA**), triethylamine (**TEA**), and ethanolamine (**EtOA**) was investigated. Each time, the addition of the pollutant leads to a diminution of the fluorescence intensity (Supporting Information, Figure S4), following the Stern−Volmer equation (eq 3).

$$\frac{I_0}{I} - 1 = K_{SV}[Q] \qquad (3)$$

The slopes of the Stern−Volmer plots (K_{SV}) are in good agreement with the electron density of each quencher (Figure 5.), which is fully consistent with a quenching by electron transfer in the excited state, as previously demonstrated with other chloroalkoxytetrazines.[19,23]

The same work was then performed for the tetrazine doped NPs (Supporting Information, Figures S5 and S6). In the case of **DPA** and **TEA** a linear Stern−Volmer plot is also obtained (Figure 6), in spite of more complex photophysical properties for grafted NPs than for free tetrazine. Although according to the resulting Stern−Volmer constants, the free dye **2** stays a better acceptor for such pollutants (Table 2.), an efficient quenching of the fluorescence of the nanoparticles is also observed. Whereas for tetrazine **2**, **DPA** is the best quencher, the fluorescence of both **NP1** and **NP2** are more efficiently quenched by **TEA** than by **DPA** (Table 2). This could be related to the steric hindrance of the pollutant, which disfavors the interaction of **DPA** with a dense layer of grafted tetrazine on NPs. For both pollutants, higher Stern−Volmer constants are observed for **NP2** than for **NP1** which can be explained by a less dense layer of fluorophores on **NP2** than on **NP1**, leading at the same time to less

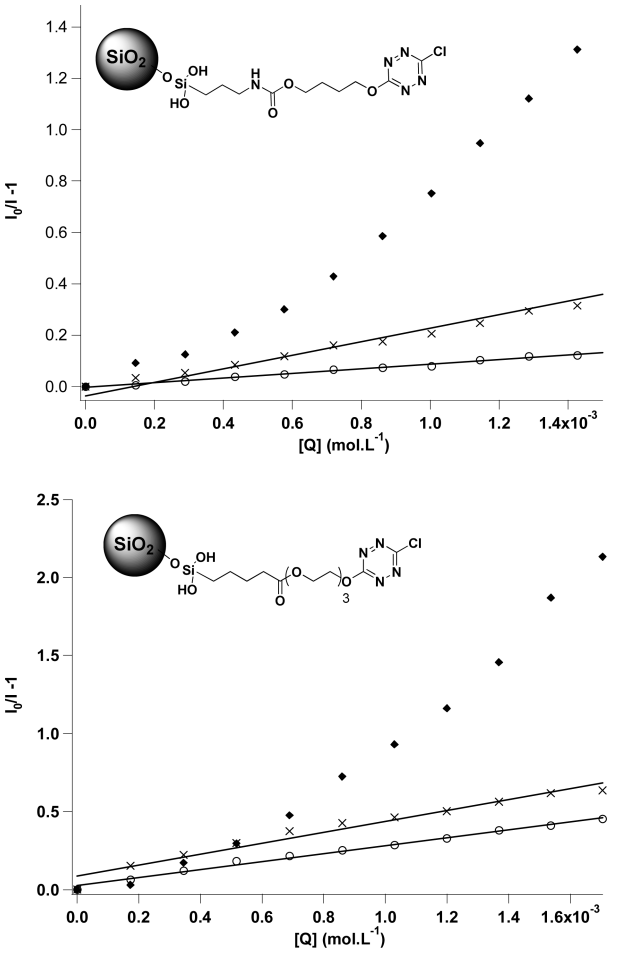

Figure 6. Stern−Volmer plots for **NP1** (top) and **NP2** (bottom) as function of quencher concentration for various quenchers: ○ **DPA**; ◆ **EtOA**; × **TEA**.

Table 2. Stern−Volmer Constants for Free Dye 2, NP1, and NP2 in the Presence of DPA, TEA, and EtOA

	K_{SV} (mol^{-1}.L)		
quencher	**2**	**NP1**	**NP2**
DPA	2050	88	277
TEA	1140	245	422
EtOA	225		

self-quenching between grafted tetrazines and to a better accessibility of tetrazines to pollutants.

After washing of the particles it is possible to reuse them, and observe again the fluorescence quenching. However unfortunately, quantitative recovery of the particle happened to be quite difficult, and therefore the baseline and absolute fluorescence emission after washing does not match the initial one (by about 10%). The reuse of particles is therefore possible, but probably presupposes probably using larger particles easier to quantitatively recover.

The fluorescence behavior upon addition of **EtOA** provided a more complicated mechanism. While this pollutant slightly quenches the fluorescence of the free dye **2** (K_{SV} = 225 mol^{-1} L), the fluorescence emission of suspensions of **NP1** and **NP2**

dx.doi.org/10.1021/cm202223w |*Chem. Mater.* 2011, 23, 4599–4605

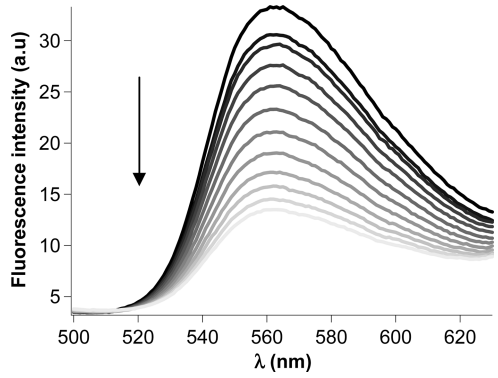

Figure 7. Emission spectra of **NP1** in the presence of increasing **EtOA** concentration (0−1.6 mM) in CH_3CN. Conditions: [dye] = 0.29 mM, λ_{exc} = 340 nm.

drastically diminishes with increasing concentration of pollutant (Figure 7). For both nanoparticles, the plot of $I_0/I - 1$ against [EtOA] deviates from linearity with an upward curvature, which indicates that static and dynamic quenching occur simultaneously. This is confirmed by time-resolved fluorescence experiment on **NP1** (Supporting Information, Figure S7) which shows both a decrease of the average fluorescence lifetime and a decrease of the initial fluorescence intensity.[28] Further experiments are in progress to understand the origin of this enhanced quenching of the nanoparticles fluorescence by ethanolamine.

■ CONCLUSIONS

Silica nanoparticles have been grafted with trialkoxysilane tetrazine dyes **2** and **4** resulting in luminescent and electroactive silica nanohybrids. The functionalized nanoparticles show a bright fluorescence emission, with emission and excitation bands typical of chloroalkoxytetrazines fluorophores, although time-resolved fluorescence studies evidence some degree of quenching because of interchromophoric interactions. The fluorescence emission of the functionalized nanoparticles has been studied in the presence of various low molecular weight amines. Extinction of the fluorescence of the nanoparticles because of photoinduced electron transfer between the photoexcited tetrazine and the amine is observed. In the case of ethanolamine, an amplification of the quenching is observed compared to free tetrazine **2** in solution. The combination of their optical and electrochemical properties makes these functionalized nanoparticles potentially useful for amine sensing. Selective detection of a given amine could be obtained by preparing an array of nanoparticles functionalized with different fluorescent tetrazines having different electron affinities. The response of each functionalized nanoparticle would depend on the tetrazine electron affinity, thus allowing a specific answer of the array to the amine of interest. Work in this direction is in progress in our laboratory. We are also currently studying the influence of the nanoparticles size on the sensing efficiency, and we are working on the preparation of bifunctional nanoparticles with enhanced optical properties.

■ EXPERIMENTAL SECTION

General Procedure. All chemical reagents and solvents were purchased from commercial sources (Aldrich, Acros, SDS) and used as received. Spectroscopic grade solvents purchased from Aldrich were used for spectroscopic measurements. Analytical TLC was performed on Kieselgel F-254 precoated plates. Visualization was done with UV lamp. Flash chromatography was carried out with silica gel 60 (230−400 mesh) from SDS. Dichlorotetrazine was synthesized according to literature procedures.[20] ^1H and ^{13}C NMR spectra were recorded on a JEOL 400 MHz spectrometer, and chemical shifts (δ) were reported in ppm relative to TMS and referenced to the residual solvent. Coupling constants (J) are reported in hertz (Hz) and refer to apparent peak multiplicities. Multiplicities are reported using the following abbreviations: s, singlet; d, doublet; t, triplet; q, quartet; m, multiplet; bs, broad singlet. IR spectra were measured with a Nicolet Avatar 330 FT-IR spectrometer. High-resolution mass spectra were performed at the East China Normal University. Elemental analyses were performed at the Service de Microanalyse de l'ICSN (CNRS, Gif-sur-Yvette, France).

*4-(3-(Triethoxysilyl)propylcarbamoyl-oxy)but-1-ol (**1**).* Triethoxy-(3-isocyanatopropyl)silane (2.7 mL, 11.1 mmol) and 1,4-butanediol (4.9 mL, 55.5 mmol, 5 equiv) were mixed in toluene (100 mL) and refluxed over 18 h. The reaction was quenched with deionized water (20 mL), extracted with EtOAc (3 × 45 mL), dried over $MgSO_4$ and concentrated under vacuum. The residue was purified by flash chromatography over silica gel (50% petroleum ether/EtOAc) to give the desired product as a colorless oil (2.36 g, 63%). ^1H NMR (400 MHz, $CDCl_3$): δ = 5.4 (bs, 1H), 4.01 (m, 2H), 3.76 (q, ^3J = 6.8 Hz, 6H), 3.59 (t, ^3J = 6.4 Hz, 2H), 3.09 (m, 2H), 1.57 (m, 6H), 1.16 (t, ^3J = 6.8 Hz, 9H), 0.56 (t, ^3J = 8.0 Hz, 2H). ^{13}C NMR (100 MHz, $CDCl_3$): δ = 156.74, 64.17, 61.47, 58.10, 43.10, 28.71, 25.30, 22.94, 17.91, 7.30 ppm. HR-MS (ESI) m/z $[M+Na]^+$ for $C_{14}H_{31}NO_6SiNa$: calcd. 360.1818, found 360.1822.

*3-Chloro-6(4-(3-(triethoxysilyl)propyl-carbamoyl-oxy) butoxy)-tetrazine (**2**).* To a solution containing compound **1** (0.67 g, 2 mmol) and dichlorotetrazine (0.3 g, 2 mmol, 1 equiv) in dry CH_2Cl_2 (50 mL) was slowly added 2,4,6-trimethylpyridine (collidine) (0.26 mL, 2 mmol, 1equiv). The reaction mixture stirred at room temperature until TLC showed disappearance of the starting materials. After 1 h, the reaction mixture was concentrated, and the residue was purified over silica gel (40% petroleum ether/EtOAc) providing a fluorescent orange oil (0.42 g, 51%). IR (neat) 1064, 1188, 1490, 1706 cm^{-1}. ^1H NMR (400 MHz, $CDCl_3$): δ = 4.96 (bs, 1H), 4.63 (t, ^3J = 6.4 Hz 2H), 4.08 (m, 2H), 3.75 (q, ^3J = 6.8 Hz, 6H), 3.11 (t, ^3J = 6.4 Hz, 2H), 1.97 (m, 2H), 1.80 (m, 2H), 1.58 (m, 2H), 1.18 (q, ^3J = 7.8 Hz, 9H), 0.57 (t, ^3J = 7.8 Hz, 2H). ^{13}C NMR (100 MHz, $CDCl_3$): δ = 166.70, 164.33, 158.56, 70.48, 63.84, 58.48, 43.44, 25.51, 25.28, 23.31, 18.33, 7.70 ppm. UV−vis (acetonitrile): λ_{max} (ε): 330 nm (3350), 515 nm (708). Φ_F = 0.26 (acetonitrile, reference: rhodamine 590, Φ_F = 0.95 in ethanol[29]). HR-MS (ESI) m/z $[M+Na]^+$ for $C_{16}H_{30}ClNO_5SiNa$: calcd. 474.1552, found 474.1515.

*2-(2-(3-(Triethoxysilyl)propylcarbamoyl-oxy-ethoxy)ethoxy)ethanol (**3**).* Triethoxy(3-isocyanatopropyl)silane (1.7 mL, 6.7 mmol) and triethyleneglycol (5 g, 33.3 mmol, 5 equiv) were mixed in toluene (100 mL) and refluxed over 18 h. The reaction was then cooled to room temperature and concentrated under vacuum. The residue was purified by flash chromatography over silica gel (50% petroleum ether/EtOAc) to give the desired product as a colorless oil (2.36 g, 63%). ^1H NMR (400 MHz, $CDCl_3$): δ = 5.23 (bs, 1H), 4.11 (t, ^3J = 4.6 Hz, 2H), 3.73 (q, ^3J = 6.9 Hz, 6H), 3.62 (m, 8H), 3.51 (t, ^3J = 4.6 Hz, 2H), 3.07 (q, ^3J = 6.9 Hz, 2H), 2.98 (bs, 1H), 1.51 (m, 2H), 1.11 (t, ^3J = 7.3 Hz, 9H), 0.53 (t, ^3J = 8.2 Hz, 2H). ^{13}C NMR (100 MHz, $CDCl_3$): δ = 156.42, 72.62, 72.47, 70.38, 69.58, 63.52, 61.55, 58.43, 43.4, 23.22, 18.26, 7.51 ppm. HR-MS (ESI) m/z $[M+Na]^+$ for $C_{16}H_{35}ClNO_8SiNa$: calcd. 420.2030, found 420.2068.

*3-Chloro-6-(2-(2-(3-(triethoxysilyl)propyl-carbamoyl-oxy-ethoxy)-ethoxy)ethoxy)-tetrazine (**4**).* To a solution containing compound **3** (1 g, 2.51 mmol) and dichlorotetrazine (0.37 g, 2.51 mmol, 1equiv) in dry CH_2Cl_2 (50 mL) was slowly added collidine (0.32 mL, 2.51 mmol, 1 equiv). The reaction mixture stirred at room temperature until TLC showed disappearance of the starting materials. After 1 h, the reaction

mixture was concentrated, and the residue was purified over silica gel (50% petroleum ether/EtOAc) providing a fluorescent orange oil (0.58 g, 45%). IR (neat) 1024, 1100, 1482, 1710 cm^{-1} .^{1}H NMR (400 MHz, $CDCl_3$): δ = 5.01 (bs, 1H), 4.79 (t, ^3J = 4.2 Hz 2H), 4.15 (m, 2H), 3.96 (t,^3J = 4.2 Hz, 2H), 3.77 (q, ^3J = 7.1 Hz, 6H), 3.69 (m, 2H), 3.63 (s, 4H), 3.12 (q ^3J = 6.6 Hz, 2H), 1.58 (m, 2H), 1.19 (t, ^3J = 7.1 Hz, 9H), 0.59 (t, ^3J = 8.2 Hz, 2H). ^{13}C NMR (100 MHz, $CDCl_3$): δ = 166.81, 164.44, 156.43, 70.90, 70.58, 69.81, 68.74, 63.73, 58.49, 43.53, 23.36, 18.34, 7.68 ppm. UV−vis (acetonitrile): λ_{max} (ε): 330 nm (3250), 515 nm (730). Φ_F= 0.28 (acetonitrile, reference: rhodamine 590, Φ_F = 0.95 in ethanol[29]). HR-MS (ESI) m/z $[M+Na]^+$ for $C_{18}H_{34}ClN_5O_8SiNa$: calcd. 534.1763, found 534.1782.

Silica Nanoparticles Preparation. The silica nanoparticles were prepared according to the Stöber protocol.[2] A solution of TEOS (14.5 mL, 64.9 mmol) and deionized water (0.8 mL) in absolute ethanol (65.7 mL) was prepared in a thermostatted vessel. After 20 min at 40 °C, ammonia (4.9 mL, 28% water solution) was quickly added to the mixture, and the reaction was vigorously stirred for 6 h. DLS analysis yielded a diameter of 135 nm for the resulting silica nanoparticles. The excess of TEOS and ammonia were eliminated by successive centrifugation and redispersion in water (3 times) and acetonitrile (3 times). The resulting silica nanoparticles were dried overnight under vacuum and stored as a powder without alteration of the particle size.

Tetrazine Doped Silica Nanoparticles. The hereinbefore prepared nanoparticles were functionalized under mild acidic conditions. A suspension of silica particle (0.6 g) in acetonitrile (20 mL) was sonicated until DLS analysis yielded to 135 nm. A dye (**2** or **4**, 0.15 mmol) solution in acetonitrile (10 mL) was mixed with glacial acetic acid (0.45 mmol, 3 equiv) and added to the silica suspension. The grafting reaction stirred at room temperature over a 24 h period. The excess of tetrazine derivative was removed by successive centrifugation and redispersion in acetonitrile provided a pink suspension of functionalized silica nanospheres.

Size Measurements. A VASCO-1 from Cordouan Technology was used for the DLS measurements. A laser beam at 658 nm (15 mW) is guided to a cell containing the sample. Fluctuations of the scattering are followed and fitted using the Stokes−Einstein equation to determine the size distribution. SEM measurements were performed on a Quanta FEG scanning electron microscope from FEI.

Electrochemical Studies. Electrochemical studies were performed using acetonitrile (SDS, anhydrous for analysis) as a solvent, with *n*-tetrabutylammonium hexafluorophosphate (Fluka, puriss.) as the supporting electrolyte. The substrate concentration was about 1 mM. A 50 μm diameter Pt microelectrode was used as the working electrode, along with a Ag^+/Ag (10^{-2} M) reference electrode and a Pt wire counter electrode. The cell was connected to a CH Instruments 600B potentiostat monitored by a PC computer. All solutions were degassed by argon bubbling prior to each experiment.

Photophysical Studies. A UV−vis Varian CARY 5 spectrophotometer equipped with an internal integrating sphere was used. Excitation and emission spectra were measured on a SPEX Fluoromax-3 (Jobin-Yvon). A right-angle configuration was used. Optical density of the samples was checked to be less than 0.1 to avoid reabsorption artifacts. The fluorescence decay curves were obtained with a time-correlated single-photon-counting method using a titanium-sapphire laser (82 MHz, repetition rate lowered to 4 MHz thanks to a pulse-picker, 1 ps pulse width, a doubling crystal is used to reach 495 nm excitation) pumped by an argon ion laser.

■ ASSOCIATED CONTENT

Ⓢ Supporting Information. Size distribution measured by DLS and SEM image of silica nanoparticles before functionalization, and fluorescence emission of the nanoparticles as a function of the grafting reaction time. Emission spectra of **2**, **NP1**, and **NP2** in the presence of increasing pollutant concentration (0−1.6 mM) in acetonitrile. This material is available free of charge via the Internet at http://pubs.acs.org.

■ AUTHOR INFORMATION

Corresponding Author

*E-mail: clemence.allain@ppsm.ens-cachan.fr (C.A.), audebert@ppsm.ens-cachan.fr (P.A.).

Author Contributions

The manuscript was written through contributions of all authors. All authors have given approval to the final version of the manuscript.

■ ACKNOWLEDGMENT

We thank the DGA (Direction Générale de l'Armement) for a PhD fellowship to J.M. D. Caldemaison and J. M. Allain (Laboratoire de Mécanique des Solides, Ecole Polytechnique, Palaiseau, France) are gratefully acknowledged for the SEM images.

■ REFERENCES

(1) Bonacchi, S.; Genovese, D.; Juris, R.; Montalti, M.; Prodi, L.; Rampazzo, E.; Zaccheroni, N. *Angew. Chem., Int. Ed.* **2011**, *50* (18), 4056–4066.

(2) Stöber, W.; Fink, A.; Bohn, E. *J. Colloid Interface Sci.* **1968**, *26*, 62–69.

(3) Van Blaaderen, A.; Vrij, A. *Langmuir* **1992**, *8*, 2921–2931.

(4) Bagwe, R. P.; Yang, C.; Hilliard, L. R.; Tan, W. *Langmuir* **2004**, *20*, 8336–8342.

(5) Rampazzo, E.; Bonacchi, S.; Montalti, M.; Prodi, L.; Zaccheroni, N. *J. Am. Chem. Soc.* **2007**, *129* (46), 14251–14256.

(6) (a) Burns, A.; Sengupta, P.; Zedayko, T.; Baird, B.; Wiesner, U. *Small* **2006**, *2* (6), 723–726. (b) Doussineau, T.; Trupp, S.; Mohr, G. J. *J. Colloid Interface Sci.* **2009**, *339* (1), 266–270. (c) Arduini, M.; Mancin, F.; Tecilla, P.; Tonellato, U. *Langmuir* **2007**, *23* (16), 8632–8636.

(7) Lu, J.; Liong, M.; Li, Z.; Zink, J. I.; Tamanoi, F. *Small* **2010**, *6*, 1794–1805.

(8) Klajn, R.; Stoddart, J. F.; Grzybowski, B. A. *Chem. Soc. Rev.* **2010**, *39*, 2203–2237.

(9) Nyffenegger, R.; Quellet, C.; Ricka, J. *J. Colloid Interface Sci.* **1993**, *159* (1), 150–157.

(10) Dewar, P. J.; MacGillivray, T. F.; Crispo, S. M.; Smith-Palmer, T. *J. Colloid Interface Sci.* **2000**, *228* (2), 253–258.

(11) Bonacchi, S.; Rampazzo, E.; Montalti, M.; Prodi, L.; Zaccheroni, N.; Mancin, F.; Teolato, P. *Langmuir* **2008**, *24* (15), 8387–8392.

(12) Montalti, M.; Prodi, L.; Zaccheroni, N. *J. Mater. Chem.* **2005**, *15*, 2810–2814.

(13) Gao, D.; Wang, Z.; Liu, B.; Ni, L.; Wu, M.; Zhang, Z. *Anal. Chem.* **2008**, *80* (22), 8545–8553.

(14) Geng, J.; Liu, P.; Liu, B.; Guan, G.; Zhang, Z.; Han, M.-Y. *Chem.—Eur. J.* **2010**, *16* (12), 3720–3727.

(15) Clavier, G.; Audebert, P. *Chem. Rev.* **2010**, *110* (6), 3299–3314.

(16) Saracoglu, N. *Tetrahedron* **2007**, *63* (20), 4199–4236.

(17) (a) Boger, D. L. *Chemtracts* **1996**, *9*, 149–189. (b) Blackman, M. L.; Royzen, M.; Fox, J. M. *J. Am. Chem. Soc.* **2008**, *130* (41), 13518–13519.(c) Devaraj, N. K.; Weissleder, R. *Acc. Chem. Res.* **2011**, *44* (9), 816−827.

(18) See for example: Joo, Y.-H.; Twamley, B.; Garg, S.; Shreeve, J. M. *Angew. Chem., Int. Ed.* **2008**, *47* (33), 6236–6239. Huynh, M. H. V.; Hiskey, M. A.; Chavez, D. E.; Naud, D. L.; Gilardi, R. D. *J. Am. Chem. Soc.* **2005**, *127* (36), 12537–12543.

(19) Audebert, P.; Miomandre, F.; Clavier, G.; Vernieres, M. C.; Badré, S.; Meallet-Renault, R. *Chem.—Eur. J.* **2005**, *11* (19), 5667–5673.

(20) Gong, Y. H.; Miomandre, F.; Meallet-Renault, R.; Badre, S.; Galmiche, L.; Tang, J.; Audebert, P.; Clavier, G. *Eur. J. Org. Chem.* **2009**, *35*, 6121–6128.
(21) Qing, Z.; Audebert, P.; Clavier, G.; Miomandre, F.; Tang, J.; Vu, T. T.; Meallet-Renault, R. *J. Electroanal. Chem.* **2009**, *632* (1−2), 39–44.
(22) Gückel, F.; Maki, A. H.; Neugebauer, F. A.; Schweitzer, D.; Vogler, H. *Chem. Phys.* **1992**, *164* (2), 217–227.
(23) Gong, Y. H.; Audebert, P.; Clavier, G.; Miomandre, F.; Tang, J.; Badre, S.; Meallet-Renault, R.; Naidus, E. *New J. Chem.* **2008**, *32* (7), 1235–1242.
(24) (a) Lu, G.; Grossman, J. E.; Lambert, J. B. *J. Org. Chem.* **2006**, *71*, 1769–1776. (b) McGrier, P. L.; Solntsev, K. M.; Miao, S.; Tolbert, L. M.; Miranda, O. R.; Rotello, V. M.; Bunz, U. H. F. *Chem.—Eur. J.* **2008**, *14* (15), 4503–4510. (c) Nakamura, M.; Sanji, T.; Tanaka, M. *Chem.—Eur. J.* **2011**, *17*, 5344–5349.
(25) van Blaaderen, A.; Vrij, A. *J. Colloid Interface Sci.* **1993**, *156*, 1–18.
(26) Calero, P.; Martinez-Manez, R.; Sancenon, F.; Soto, J. *Eur. J. Inorg. Chem.* **2008**, 5649–5658.
(27) (a) Beasley, C. A.; Murray, R. W. *Langmuir* **2009**, *25*, 10370. (b) Budny, A.; Nowak, F.; Plumeré, N.; Schetter, B.; Speiser, B.; Straub, D.; Mayer, H. A.; Reginek, M. *Langmuir* **2006**, *22*, 10605.
(28) Valeur, B. *Molecular Fluorescence: Principles and Applications*; Wiley-VCH Verlag GmbH: Weinheim, Germany, 2001.
(29) Kubin, R. F.; Fletcher, A. N. *J. Lumin.* **1982**, *27*, 455–462.